

region (Fig. 3) could be attributed to the sum of basal and tip polymerization. We modeled relative contribution of tip and basal polymerization to the measured steady-state filament distribution (Fig. 4B). Our results show that polymerization away from the tip generates most of the actin filaments in lamellipodia, consistent with the rapid recovery kinetics of photoactivation experiments (8–10).

These findings will need to be considered in the context of the specific geometric constraints of the leading edge. Tip polymerization might be promoted by factors attached to the lamellipodium tip such as WAVE/Scar, VASP/Mena, and focal adhesion complexes (28–30). Alternatively, tip polymerization could be governed by physical restriction, if the force between the filament end and the plasma membrane regulates filament elongation (31, 32).

Much less is known about how basal polymerization might be regulated, despite its dominant role in determining total filament distribution (Fig. 4B). To accomplish fast basal polymerization, newly growing ends must be continuously generated in the lamellipodium body by some combination of nucleation, severing, uncapping, and shrinking to growing transitions. Such growing ends may affect leading-edge dynamics, extending filaments toward the lamellipodium tip. Potential regulatory mechanisms for basal polymerization include uncapping by phosphoinositides (33) and severing by cofilin (34). Single-molecule analysis of actin regulatory proteins should help determine the role of these pathways and deepen our understanding of the dynamic organization of actin arrays.

References and Notes

1. T. D. Pollard, L. Blanchoin, R. D. Mullins, *Annu. Rev. Biophys. Biomol. Struct.* **29**, 545 (2000).
2. D. Pantaloni, C. Le Clairche, M. F. Carlier, *Science* **292**, 1502 (2001).
3. L. P. Cramer, *Curr. Biol.* **9**, 1095 (1999).
4. J. R. Bamberg, *Annu. Rev. Cell. Dev. Biol.* **15**, 185 (1999).
5. S. Okabe, N. Hirokawa, *J. Cell Biol.* **109**, 1581 (1989).
6. M. H. Symons, T. J. Mitchison, *J. Cell Biol.* **114**, 503 (1991).
7. Y. L. Wang, *J. Cell Biol.* **101**, 597 (1985).
8. J. A. Theriot, T. J. Mitchison, *Nature* **352**, 126 (1991).
9. ———, T. J. Mitchison, *J. Cell Biol.* **119**, 367 (1992).
10. A. Mallavarapu, T. Mitchison, *J. Cell Biol.* **146**, 1097 (1999).
11. M. Bailly *et al.*, *J. Cell Biol.* **145**, 331 (1999).
12. Y. Tardy, J. L. McGrath, J. H. Hartwig, C. F. Dewey, *Biophys. J.* **69**, 1674 (1995).
13. Decay rates of signals marked by photoactivation and photobleaching do not correspond with actin depolymerization rates at fast actin turnover rates (g) and at high polymer-to-monomer ratios of actin (Cf:cm) (12). From high concentration of filaments, $\sim 1000 \mu\text{M}$ (20), and our observations using the F-actin-preserving extraction method (16), it was estimated that Cf:cm might exceed 5:1 in lamellipodia. Simulation using the Tardy model (12) estimated that the decay rate of uncaged actin label was about one-half the depolymerization rate at Cf:cm = 5, $g = 0.03$ (this study), and $D = 5 \times 10^{-8} \text{ cm}^2/\text{s}$ (20).
14. C. M. Waterman-Storer, E. D. Salmon, *J. Cell Biol.* **139**, 417 (1997).
15. ———, *Biophys. J.* **75**, 2059 (1998).

16. Supplementary material is available on Science Online at www.sciencemag.org/cgi/content/full/295/5557/1083/DC1
17. C. Ballestrem, B. Wehrle-Haller, B. A. Imhof, *J. Cell Sci.* **111**, 1649 (1998).
18. M. Boshart *et al.*, *Cell* **41**, 521 (1985).
19. V. C. Abraham, V. Krishnamurthi, D. L. Taylor, F. Lanni, *Biophys. J.* **77**, 1721 (1999).
20. J. L. McGrath, Y. Tardy, C. F. Dewey Jr., J. J. Meister, J. H. Hartwig, *Biophys. J.* **75**, 2070 (1998).
21. The lifetime distribution of actin filaments differs from an exponential failure distribution (Fig. 2E), as assumed in photoactivation studies. However, approximating the regression data with a single exponential curve is useful for estimating the overall actin depolymerization rate from a limited number of images (Fig. 2, B and C).
22. M. R. Bubb, I. Spector, B. B. Beyer, K. M. Fosen, *J. Biol. Chem.* **275**, 5163 (2000).
23. R. M. Dickson, A. B. Cubitt, R. Y. Tsien, W. E. Moerner, *Nature* **388**, 355 (1997).
24. R. D. Mullins, J. A. Heuser, T. D. Pollard, *Proc. Natl. Acad. Sci. U.S.A.* **95**, 6181 (1998).

25. L. Blanchoin, T. D. Pollard, R. D. Mullins, *Curr. Biol.* **10**, 1273 (2000).
26. D. J. Kwiatkowski, *Curr. Opin. Cell Biol.* **11**, 103 (1999).
27. S. E. Hitchcock-DeGregori, P. Sampath, T. D. Pollard, *Biochemistry* **27**, 9183 (1988).
28. P. Hahne, A. Sechi, S. Benesch, J. V. Small, *FEBS Lett.* **492**, 215 (2001).
29. H. Nakagawa *et al.*, *J. Cell Sci.* **114**, 1555 (2001).
30. N. A. Hotchin, A. Hall, *J. Cell Biol.* **131**, 1857 (1995).
31. C. S. Peskin, G. M. Odell, G. F. Oster, *Biophys. J.* **65**, 316 (1993).
32. A. Mogilner, G. Oster, *Biophys. J.* **71**, 3030 (1996).
33. J. H. Hartwig *et al.*, *Cell* **82**, 643 (1995).
34. A. Y. Chan, M. Bailly, N. Zebra, J. E. Segall, J. S. Condeelis, *J. Cell Biol.* **148**, 531 (2000).
35. Supported by NIH grant, GM48027, and by Research Fellowship of Uehara Memorial Foundation (N.W.). We thank R. Li and T. Walz for critical reading of the manuscript, and we thank members of the laboratory, especially W. M. Brieher, for helpful discussions.

24 October 2001; accepted 4 January 2002

Generation of an LFA-1 Antagonist by the Transfer of the ICAM-1 Immunoregulatory Epitope to a Small Molecule

T. R. Gadek,^{1*} D. J. Burdick,^{1*} R. S. McDowell,^{1†} M. S. Stanley,¹ J. C. Marsters Jr.,¹ K. J. Paris,¹ D. A. Oare,^{1‡} M. E. Reynolds,¹ C. Ladner,² K. A. Zioncheck,² W. P. Lee,² P. Gribling,² M. S. Dennis,³ N. J. Skelton,³ D. B. Tumas,⁴ K. R. Clark,⁵ S. M. Keating,⁵ M. H. Beresini,⁵ J. W. Tilley,⁶ L. G. Presta,⁷ S. C. Bodary²

The protein-protein interaction between leukocyte functional antigen-1 (LFA-1) and intercellular adhesion molecule-1 (ICAM-1) is critical to lymphocyte and immune system function. Here, we report on the transfer of the contiguous, nonlinear epitope of ICAM-1, responsible for its association with LFA-1, to a small-molecule framework. These LFA-1 antagonists bound LFA-1, blocked binding of ICAM-1, and inhibited a mixed lymphocyte reaction (MLR) with potency significantly greater than that of cyclosporine A. Furthermore, in comparison to an antibody to LFA-1, they exhibited significant anti-inflammatory effects in vivo. These results demonstrate the utility of small-molecule mimics of nonlinear protein epitopes and the protein epitopes themselves as leads in the identification of novel pharmaceutical agents.

The interaction of LFA-1 (the integrin $\alpha\text{L}\beta\text{2}$, CD11a /CD18) with the ICAM proteins 1, 2, and 3 is critical to the adhesion, extravasa-

tion, migration, and proliferation of lymphocytes (1–3). Antibodies directed against the CD11a subunit of LFA-1, which block the binding of its native protein ligand, ICAM-1, have been shown to safely and effectively moderate lymphocyte function in various animal models of human diseases (4–6). Humanized antibodies (7) have been advanced into clinical trials for the treatment of psoriasis and transplant rejection (8, 9). The safety and efficacy observed in these studies has validated LFA-1 as a therapeutic target of interest to the pharmaceutical industry.

An epitope comprising residues E34, K39, M64, Y66, N68, and Q73 (10) within ICAM-1's first domain has been identified as essen-

Departments of ¹Bioorganic Chemistry, ²Immunology, ³Protein Engineering, ⁴Pathology, ⁵Small Molecule Pharmacology, and ⁷Antibody Technology, Genentech, One DNA Way, South San Francisco, CA 94080, USA. ⁶Roche Research Center, Hoffmann-La Roche, Nutley, NJ 07110, USA.

*To whom correspondence should be addressed. E-mail: trg@gene.com (T.R.G.); burdick.dan@gene.com (D.J.B.)

†Present address: Sunesis Pharmaceuticals, 341 Oyster Point Boulevard, South San Francisco, CA 94080, USA.

‡Present address: Gilead Sciences, 333 Lakeside Drive, Foster City, CA 94404, USA.

REPORTS

tial for its interaction with LFA-1 (11, 12). The function of this epitope is embedded in the carboxylic acid, amine, sulfide, phenol, and carboxamide chemical functionalities of the amino acid side chains of these six residues and their display in three dimensions along one face of the protein. We supposed that molecules which mimicked this epitope could capture the LFA-1 binding specificity and safety inherent in ICAM-1's function as a regulator of the immune system. Traditional methods generally use a small molecule, known to bind and block the function of a target, as a "lead" in the generation of pharmaceuticals. In contrast, we sought to use LFA-1's native ligand, ICAM-1, as a lead in the identification of novel small-molecule immunosuppressive agents. The minimum criteria for these agents would be to prevent the association of LFA-1 and ICAM-1 and potentially block lymphocyte function and regulate human T cell-mediated inflammation in a manner similar to the humanized antibodies to CD11a (anti-CD11a).

The challenge in the use of a protein, such as ICAM-1, as a lead to a pharmaceutical is the discontinuous nature of its binding epitope spanning 40 residues. Although these residues are not proximal in primary sequence, they are presented in a contiguous fashion by the tertiary fold of ICAM-1, which reduces the α -carbon distances between key residues to a range falling within the dimensions of a small molecule. We envisioned a design and discovery process, which would seek to identify molecular frameworks capable of reproducing the C α coordinates and acquiring the C α -C β vectors of E34, K39, M64, Y66, N68, and Q73. For simplicity, we chose to initially focus on the mimicry of two residues with the expectation that we could include additional aspects of the epitope after we had successfully identified a molecule which bound LFA-1 and blocked its binding to ICAM-1.

Preliminary ICAM-1 mutagenesis showed that the first domain residues E34 and K39 were critical for LFA-1 binding (11, 13), and a homology model indicated that these residues opposed each other on the C-D strands of an antiparallel β -sheet (11, 14). Molecular modeling suggested that the simplest approach to mimicking these residues would be to traverse the face of the model's β -sheet from α -carbon to α -carbon, crossing the H-bond network between the strands, rather than following the main-chain connectivity around the proposed C-D loop. We recognized that a flexible RXD amino acid sequence could fit our design criteria and found that kistrin, a disintegrin protein containing an RGD sequence (15, 16) inhibited the binding of LFA-1 and ICAM-1 in vitro (Table 1) and blocked the homing of murine lymphocytes in vivo (17). Alanine mutagenesis (18) identified a linear RGDMP epitope within

kistrin and developed a structure activity relationship (SAR) consistent with kistrin as a mimic of E34 and K39 from ICAM-1. This sequence was studied in the context of a series of cyclic peptides including the disulfide H₂N-CRGMPC-COOH. Alanine analogs indicated the necessity of a carboxylic acid moiety for LFA-1 binding and the relative unimportance of the arginine residue in this peptide. Further analysis in a library of H₂N-CXXDMPC-COOH disulfides identified H₂N-CGFDMPC-COOH (Table 1), and ultimately H₂N-CGY^(m)DMPC-COOH, (Y^(m) = *meta*-tyrosine) with binding affinity similar to kistrin and an SAR more pronounced in its sensitivity to substitutions of the phenol or COOH-terminal carboxylic acid moieties than was seen for any substitution in ICAM-1, kistrin, or the RGD peptides. Nuclear magnetic resonance and molecular modeling studies defined the bioactive conformation of H₂N-CGY^(m)DMPC-COOH (Web fig. 2). This provided the structural component of a structure activity relationship linking the epitope of H₂N-CGY^(m)DMPC-COOH to ICAM-1's epitope (14).

Work was initiated to graft the H₂N-CGY^(m)DMPC-COOH epitope onto a non-peptide template, which was expected to overcome the pharmaceutical limitations of peptides, particularly their inefficient delivery via an oral route. Similar de novo small-molecule design efforts had been successful in the past from a similarly sized peptide (19–21). While these design studies were under way, *ortho*-bromobenzoyl tryptophan (designated compound 1 in Table 1 and Fig. 1) was identified as an inhibitor of LFA-1 in

a selectivity counter-screen from a related program (22). This relatively simple molecule exhibited both potency and structural similarities with H₂N-CGY^(m)DMPC-COOH. Analogs indicated that this activity depended on a sterically bulky substituent at the *ortho* position of the benzoyl ring, thus enforcing a twist between that ring and the neighboring amide group. A similar twist was observed between the proline ring and COOH-terminal cysteine residues in the bioactive conformation of H₂N-CGY^(m)DMPC-COOH (Web fig. 2). An alignment of the carboxylic acids of compound 1 and the peptide COOH-terminus (14) further suggested that the bromo group of compound 1 could occupy the volume of the peptide's proline side chain, and that a three-atom extension at the 4-position of the benzoyl ring could be used to present the *meta*-phenol group of H₂N-CGY^(m)DMPC-COOH. For synthetic ease (23), this was first achieved with the amide linkage of the chlorine containing compound 2 (Table 1). We believe the 30-fold improvement in the inhibition of LFA-1/ICAM-1 binding achieved with the first compound synthesized in this series substantiates the structural rationale leading to the design of compound 2 from H₂N-CGY^(m)DMPC-COOH.

For the purpose of optimization, the non-peptide compounds were subdivided into five modules (Fig. 1) and modifications were subsequently made within each module to explore a chemically diverse set of substituents (Fig. 1C). The properties of any molecule can be seen as the sum of the properties of its modular parts. Consequently, the best molecules were expected to emerge from this op-

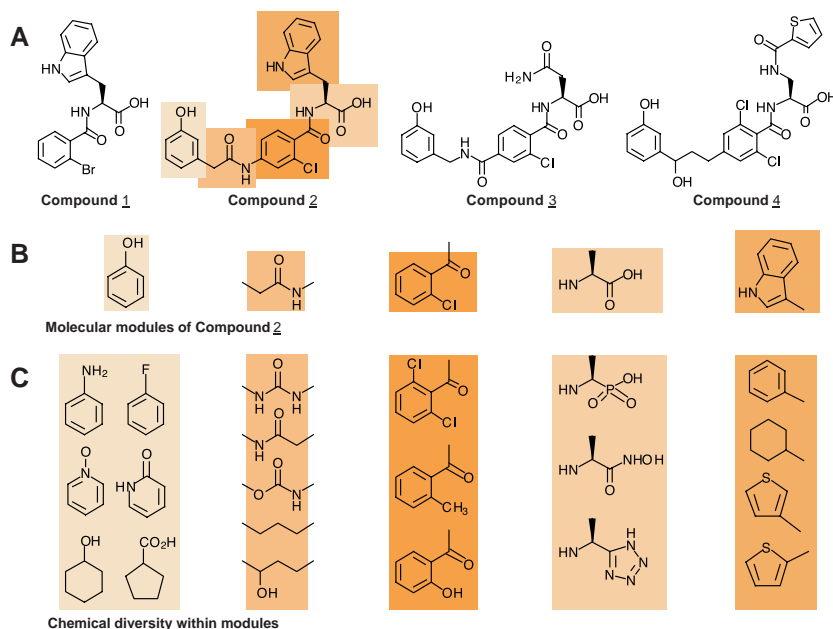


Fig. 1. The structures of (A) compounds 1 through 4. (B) The molecular modules derived from compound 2. (C) Examples of the chemical diversity explored within each module. Additional examples of chemical diversity can be found in (23).

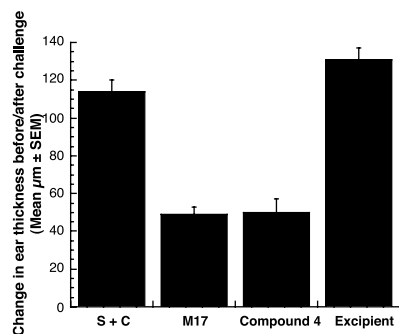


Fig. 2. Inhibition of DNFB-induced contact hypersensitivity by the anti-CD11a (M17) and compound **4**. Mice were sensitized and challenged (S+C) with DNFB and treated with M17, compound **4** or excipient (water) 3 days after sensitization (14). Bars represent the change in ear thickness before and after challenge. $P < 0.0001$ for groups treated with M17 and compound **4** compared to S+C animals.

timization process with properties that were the sum of the properties of the best individual modules. The total diversity explored by only 40 possibilities at each module would be represented in a library of $>10^8$ combinations. However, because the synthesis of such a large number of compounds was neither necessary nor feasible, we focused on combinations of the best of the more than 40 substituents introduced at each module.

Multiple series of compounds were synthesized which examined chemical diversity within a single module while holding the remaining modules constant. Furthermore, several analogous series of compounds were prepared which examined the same chemical diversity within a single module in the context of several defined combinations of the other modules. Compounds were evaluated for potency in the LFA-1/ICAM-1 enzyme-linked immunosorbent assay (ELISA), and in general, the best substituent at each module was present in the most potent compound in several analogous series of compounds. The chemical diversity exploration within a module was guided by considerations of the function of that module with respect to binding to LFA-1 (e.g., H-bonding, charge, steric bulk, and so forth) and our structural understanding of the epitopes of ICAM-1 and $\text{H}_2\text{N-CGY}^{(m)}$ DMPC-COOH. Two particularly interesting molecules emerged from this effort (Table 1). Compound **3** represents a minimal display of the epitope with high potency and compound **4** represents one of the best combinations of the best molecular modules. It is interesting to note that compounds **3** and **4** retained both the *meta*-phenol and L-amino acid functionalities of $\text{H}_2\text{N-CGY}^{(m)}$ DMPC-COOH.

Compounds **1** through **4** were compared in potency to cyclosporine A and the Fab fragment of anti-CD11a in two in vitro assays believed to be predictive of in vivo activity (Table 1). The MLR assay was used to dif-

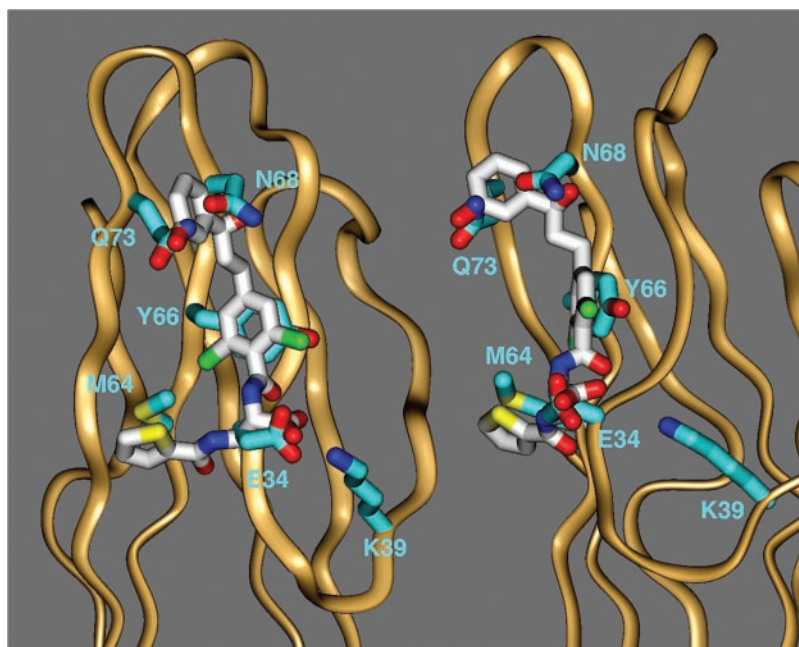


Fig. 3. Two orthogonal views of the superimposition of compound **4** on the crystal structure of the first domain of ICAM-1 (29) indicating that compound **4** mimics the ICAM-1 epitope. Residues highlighted in blue contribute significantly to LFA-1 binding. The E34 side chain of ICAM-1 has been rotated to a low-energy conformation to enhance the overlay with compound **4**.

Table 1. Comparison of the inhibition of ICAM-1/LFA-1 binding and the inhibition of mixed lymphocyte reaction (MLR). IC_{50} values were determined from a 4P fit of data from titrations over concentrations of 10^{-3} to 10^{-10} M. Values reported are the mean \pm standard deviation for $n > 2$ of experiments run in triplicate. The MLR is described in (7, 23). See Fig. 1 for the structures of compounds **1** through **4**. ND, not determined. NA, not applicable.

Substance	LFA-1 ELISA IC_{50} (μM)	MLR IC_{50} (μM)
Kistrin	0.70 ± 0.21	40*
$\text{H}_2\text{N-CRGMPC-COOH}$	207 ± 69	ND
$\text{H}_2\text{N-CGFMPC-COOH}$	13 ± 3.2	ND
$\text{H}_2\text{N-CGY}^{(m)}\text{DMPC-COOH}^\dagger$	1.6 ± 0.1	ND
Compound 1	1.4 ± 0.7	ND
Compound 2	0.047 ± 0.014	10.3 ± 6.3
Compound 3	0.0037 ± 0.0015	1.33 ± 1.1
Compound 4	0.0014 ± 0.00014	0.003 ± 0.002
Cyclosporine A	NA ‡	0.061 ± 0.034
MHM 24 Fab §	0.0023 ± 0.0001	0.020 ± 0.008

*Incomplete titration, value estimated at 50% inhibition. $^\dagger\text{Y}^{(m)}$ = *meta*-tyrosine. ‡ The immunosuppressive activity of cyclosporine does not involve its direct binding to LFA-1 or ICAM-1. § MHM 24 Fab is the Fab fragment of the murine anti-human antibody recognizing LFA-1's CD11a subunit (7).

ferentiate compounds **3** and **4**, which were similar in potency in the LFA-1/ICAM-1 ELISA. Unlike the ELISA where a median inhibitory concentration (IC_{50}) is reflective of 50% occupancy of LFA-1, the MLR is a measure of lymphocyte function under polyvalent, high-avidity conditions and requires a high level of LFA-1 occupancy for inhibition. Thus, activity in the MLR assay may predict a compound's effectiveness in disease states where a level of LFA-1 occupancy approaching 100% was required for biological efficacy (8). In the MLR, compound **4** is seven times more potent than the Fab fragment of a humanized anti-CD11a (7), 20 times more po-

tent than cyclosporine A, and >400 times more potent than compound **3**. This dramatic increase in potency between compounds **3** and **4** occurred in the first generation of compounds combining the best of the substituents within each of the five modules.

The efficacy of compound **4** was compared to anti-CD11a (6) in the lymphocyte mediated murine contact hypersensitivity model (3, 23) (Fig. 2). Efficacy equivalent to a maximal anti-CD11a response was observed when compound **4** was administered continuously over a 3-day period beginning 3 days after sensitization and 2 days before challenge with DNFB. Collectively, these

data demonstrate that compound **4** is a potent LFA-1 antagonist, which binds LFA-1, blocks the binding of ICAM-1, and inhibits LFA-1 mediated lymphocyte proliferation and adhesion *in vitro*. It achieves this with a potency significantly greater than cyclosporine A, and demonstrates its equivalence to anti-CD11a in the level of its inhibition of the immune system's response *in vivo*.

Compounds **1** through **4** emerged from considerations of the ICAM-1 epitope via kistrin, the RGDMP peptides and H₂N-CGY^(m)DMPC-COOH. Each of these LFA-1 ligands was able to compete with a fluorescein-conjugated analog of compound **3** for LFA-1 binding. SAR similarities suggest a common presentation of a carboxylic acid moiety to a binding site on LFA-1 as the basis of this competition. A comparison of the structures and molecular functionality of compound **4** and ICAM-1 responsible for their LFA-1 binding reveals that the carboxylic acid, sulfide, phenol, and carboxamide groups of the ICAM-1 epitope are embodied in compound **4** (Fig. 3) (14). This allows us to propose that compounds **2** through **4** are mimics of ICAM-1 resulting from the transfer of the ICAM epitope to a small molecule. A definitive proof of this mimicry will require the determination of the structures of LFA-1 and its complexes with ICAM-1 and compounds **2** through **4**.

We believe the work presented here (23, 24) represents the first reduction of a nonlinear, discontinuous but contiguous protein epitope (encompassing five residues spanning three different β strands across the face of a protein surface) from a protein to a small molecule. In contrast to more traditional approaches, this rational, structurally directed hypothesis and information driven lead discovery process utilized molecular modeling and structure activity relationships to identify pharmacophoric similarities within ICAM-1, kistrin, the peptides, and ultimately compounds **1** through **4**. This provided the perspective to recognize compound **1** as a viable lead and rapidly elaborate it into compounds **2** through **4**, and demonstrates the value of antibodies, protein mutagenesis, and structural (SAR) data for native protein ligands as leads in the identification of pharmaceutical agents, which block large protein-protein interactions. What remains to be seen with these small-molecule LFA-1 antagonists is a clinical evaluation of their safety and effectiveness in the control of human diseases relative to humanized anti-CD11a and other small-molecule agents discovered by other means (25–28).

References and Notes

1. R. W. McMurray, *Semin. Arthritis Rheumatism* **25**, 215 (1996).
 2. J. H. Spragg, in *Molecular Biology of Cell Adhesion Molecules*, M. A. Horton, Ed. (Wiley, New York, 1996), chap. 8, pp. 131–154.
 3. N. Oppenheimer-Marks, P. E. Lipsky, *Clin. Immunol. Immunopathol.* **79**, 203 (1996).

4. M. K. Connolly, E. A. Kitchens, B. Chan, P. Jardieu, D. Wofsy, *Clin. Immunol. Immunopathol.* **72**, 198 (1994).
 5. K. Kakimoto *et al.*, *Cell. Immunol.* **142**, 326 (1992).
 6. E. K. Nakakura *et al.*, *Transplantation* **55**, 412 (1993).
 7. W. A. Werther *et al.*, *J. Immunol.* **157**, 4986 (1996).
 8. A. Gottlieb *et al.*, *J. Am. Acad. Dermatol.* **42**, 428 (2000).
 9. H. Granlund, in *Curr. Opin. Anti-Inflammatory Immunomodulatory Invest. Drugs* **2**, 332 (2000).
 10. Single-letter abbreviations for the amino acid residues are as follows: A, Ala; C, Cys; D, Asp; E, Glu; F, Phe; G, Gly; H, His; I, Ile; K, Lys; L, Leu; M, Met; N, Asn; P, Pro; Q, Gln; R, Arg; S, Ser; T, Thr; V, Val; W, Trp; and Y, Tyr. X indicates any residue.
 11. K. L. Fisher *et al.*, *Mol. Biol. Cell* **8**, 501 (1997).
 12. J. M. Casasnovas, T. Stehle, J.-h. Liu, J.-h. Wang, T. A. Springer, *Proc. Natl. Acad. Sci. U.S.A.* **95**, 4134 (1998).
 13. D. E. Staunton, M. L. Dustin, H. P. Erickson, T. A. Springer, *Cell* **61**, 243 (1990).
 14. Supplementary material is available at Science Online at www.sciencemag.org/cgi/content/full/295/5557/1086/DC1
 15. M. S. Dennis *et al.*, *Proc. Natl. Acad. Sci. U.S.A.* **87**, 2471 (1989).
 16. M. Adler, P. Carter, R. A. Lazarus, G. Wagner, *Biochemistry* **32**, 282 (1993).
 17. S. C. Bodary, P. Gribling, W. P. Lee, unpublished data.
 18. M. S. Dennis, P. Carter, R. A. Lazarus, *Proteins Struct. Funct. Genet.* **15**, 312 (1993).
 19. R. S. McDowell *et al.*, *J. Am. Chem. Soc.* **116**, 5069 (1994).
 20. R. S. McDowell, T. R. Gadek, *J. Am. Chem. Soc.* **114**, 9245 (1992).
 21. R. S. McDowell *et al.*, *J. Am. Chem. Soc.* **116**, 5077 (1994).
 22. D. J. Burdick, in *PCT Int. Appl.* (Genentech, USA). WO 9949856 (1999), p. 9.
 23. Experimental methods for an LFA-1 ELISA assay (p. 65), the mixed lymphocyte reaction (MLR) (p. 67) and the synthesis of compounds **2** through **4** (p. 68) are found in D. J. Burdick, *PCT Int. Appl.* (Genentech, USA). WO 9949856 (1999).
 24. In the course of the studies presented here, several reports appeared describing small molecule antagonists of LFA-1/ICAM (25–27). Two have identified compounds which interact with LFA-1's allosteric I domain site (26, 27). Preliminary studies with compound **4** indicate that it binds at a different site on LFA-1, and that the allosteric site antagonist(s) do not inhibit the binding of compound **4** to LFA-1.
 25. T. A. Kelly *et al.*, *J. Immunol.* **163**, 5173 (1999).
 26. J. Kallen *et al.*, *J. Mol. Biol.* **292**, 1 (1999).
 27. G. Liu *et al.*, *J. Med. Chem.* **44**, 1202 (2001).
 28. G. Liu, *Expert Opin. Ther. Patents* **11**, 1383 (2001).
 29. J. Bella, P. R. Kolatkar, C. W. Marlor, J. M. Greve, M. G. Rossman, *Proc. Natl. Acad. Sci. U.S.A.* **95**, 4140 (1998).
 30. We thank P. Barker, C. Quan, J. Tom, and M. Struble for help with peptide synthesis and compound purification, S. Spencer for protein preparation and purification, and J. Burnier, R. Lazarus, and R. G. Hammonds for helpful discussions in the preparation of the manuscript.

17 September 2001; accepted 20 December 2001

Production of α -1,3-Galactosyltransferase Knockout Pigs by Nuclear Transfer Cloning

Liangxue Lai,¹ Donna Kolber-Simonds,³ Kwang-Wook Park,¹ Hee-Tae Cheong,^{1,4} Julia L. Greenstein,³ Gi-Sun Im,^{1,5} Melissa Samuel,¹ Aaron Bonk,¹ August Rieke,¹ Billy N. Day,¹ Clifton N. Murphy,¹ David B. Carter,^{1,2} Robert J. Hawley,³ Randall S. Prather^{1*}

The presence of galactose α -1,3-galactose residues on the surface of pig cells is a major obstacle to successful xenotransplantation. Here, we report the production of four live pigs in which one allele of the α -1,3-galactosyltransferase locus has been knocked out. These pigs were produced by nuclear transfer technology; clonal fetal fibroblast cell lines were used as nuclear donors for embryos reconstructed with enucleated pig oocytes.

Clinical transplantation has become one of the preferred treatments for end-stage organ failure since the introduction of chronic immunosuppressive drugs in the mid-1980s.

One of the novel approaches to dealing with the limited supply of human organs is the use of alternative species as a source of organs (xenotransplantation). The pig is considered the primary alternative species because of ethical considerations, breeding characteristics, infectious disease concerns, and its compatible size and physiology (1).

A major barrier to progress in pig-to-primate organ transplantation is the presence of terminal α -1,3-galactosyl (Gal) epitopes on the surface of pig cells. Humans and Old World monkeys have lost the corresponding galactosyltransferase activity in the course of

¹Department of Animal Science, ²Department of Veterinary Pathobiology, University of Missouri, Columbia, MO 65211, USA. ³Immerge BioTherapeutics Inc., Charlestown, MA 02129, USA. ⁴Department of Veterinary Medicine, College of Animal Resource Science, Kangwon National University, Chunchon 200-701, Korea. ⁵National Livestock Research Institute, Suwon 441-350, Korea.

*To whom correspondence should be addressed. E-mail: pratherR@missouri.edu